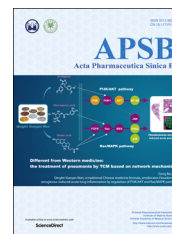




Chinese Pharmaceutical Association
Institute of Materia Medica, Chinese Academy of Medical Sciences

Acta Pharmaceutica Sinica B

www.elsevier.com/locate/apsb
www.sciencedirect.com



ORIGINAL ARTICLE

Study on four polymorphs of bifendate based on X-ray crystallography



Jinju Nie, Dezhi Yang, Kun Hu, Yang Lu*

Beijing City Key Laboratory of Polymorphic Drugs, Center of Pharmaceutical Polymorphs, Institute of Materia Medica, Chinese Academy of Medical Sciences and Peking Union Medical College, Beijing 100050, China

Received 16 February 2016; received in revised form 9 March 2016; accepted 15 March 2016

KEY WORDS

Bifendate;
Polymorphism;
Solvatomorphism;
Single-crystal structure;
Thermal analysis;
FT-IR

Abstract Bifendate, a synthetic anti-hepatitis drug, exhibits polycrystalline mode phenomena with 2 polymorphs reported (forms A and B). Single crystals of the known crystalline form B and 3 new crystallo-solvates involving bifendate solvated with tetrahydrofuran (C), dioxane (D), and pyridine (E) in a stoichiometric ratio of 1:1 were obtained and characterized by X-ray crystallography, thermal analysis, and Fourier transform infrared (FT-IR) spectroscopy. The differences in molecular conformation, intermolecular interaction and crystal packing arrangement for the four polymorphs were determined and the basis for the polymorphisms was investigated. The rotation of single bonds resulted in different orientations for the biphenyl, methyl ester and methoxyl groups. All guest solvent molecules interacted with the host molecule *via* an interesting intercalative mode along the [1 0 0] direction in the channel formed by the host molecules through weak aromatic stacking interactions or non-classical hydrogen bonds, of which the volume and planarity played an important role in the intercalation of the host with the guest. The incorporation of solvent-augmented rotation of the C–C bond of the biphenyl group had a striking effect on the host molecular conformation and contributed to the formation of bifendate polymorphs. Moreover, the simulated powder X-ray diffraction (PXRD) patterns for each form were calculated on the basis of the single-crystal data and proved to be unique. The single-crystal structures of the four crystalline forms are reported in this paper.

© 2016 Chinese Pharmaceutical Association and Institute of Materia Medica, Chinese Academy of Medical Sciences. Production and hosting by Elsevier B.V. This is an open access article under the CC BY-NC-ND license (<http://creativecommons.org/licenses/by-nc-nd/4.0/>).

Abbreviations: ADPs, anisotropic displacement parameters; ALT, alanine transaminase; CCDC, Cambridge crystallographic data center; DDB, dimethyl dimethoxy biphenyl dicarboxylate; DSC, differential scanning calorimetry; FT-IR, Fourier transform infrared spectroscopy; MW, molecular weight; PXRD, powder X-ray diffraction; SCXRD, single-crystal X-ray diffraction; TGA, thermal gravimetric analyzer.

*Corresponding author. Tel.: +86 10 63165212.

E-mail address: luy@imm.ac.cn (Yang Lu).

Peer review under responsibility of Institute of Materia Medica, Chinese Academy of Medical Sciences and Chinese Pharmaceutical Association.

<http://dx.doi.org/10.1016/j.apsb.2016.03.006>

2211-3835 © 2016 Chinese Pharmaceutical Association and Institute of Materia Medica, Chinese Academy of Medical Sciences. Production and hosting by Elsevier B.V. This is an open access article under the CC BY-NC-ND license (<http://creativecommons.org/licenses/by-nc-nd/4.0/>).

1. Introduction

Polycrystalline phenomena with solvates are not uncommon for many known drugs. The incorporation of solvent molecules results in the formation of new crystalline forms. This has attracted the attention of drug researchers. It is well known that the polymorphs of a substance are chemically identical but can differ significantly in their pharmaceutically relevant properties, such as solubility^{1,2}, dissolution rate³, and density, which can affect their bioavailability, membrane permeability⁴ and efficacy in drug formulations⁵. The term “polymorphism” describes a phenomenon in which crystal structures of a substance are defined by different unit cells, and yet each of the forms has the same elemental composition. Along this same line, “solvatomorphism” encompasses crystals of a substance defined by different unit cells, but these unit cells differ in their elemental composition through the inclusion of solvent molecules⁶. For greater insight into the regularities of solvents in crystal lattices, single-crystal X-ray diffraction (SCXRD) is suitable for detecting solvent structure and molecular interactions with the drug substance, and is particularly useful in the research of polymorphs⁷. In drug development, the formation of solvates has some relationship with the drug's preparation and production⁸, and guest solvent molecules contribute significantly to the stabilization of crystalline samples and their molecular conformation⁹. For instance, solvated forms of paclitaxel, an anticancer drug, were found to be useful intermediates¹⁰. Solvates can also be used as the medicinal forms in clinical treatment. For example, cabazitaxel, another anticancer drug, is a 1:1 acetone solvate (form A) as a commercially available raw material¹¹.

This paper focuses on the well-known drug bifendate (dimethyl-4,4'-dimethoxy-5,6,5',6'-dimethylenedioxybiphenyl-2,2'-dicarboxylate, Fig. 1A), a synthetic hepatoprotective agent derived from schisandrins^{12,13}. Bifendate displays a remarkable hepatoprotective ability against chemical liver injury induced by tetrachloride or ethanol as well as other solvents¹⁴ by lowering alanine transaminase (ALT) activity and protecting the liver in patients^{15,16}, and is widely used for the management of chronic hepatitis in China^{17–19}. Bifendate exhibits the phenomenon of polymorphism. However, to date, only two polymorphs of bifendate with melting point values of 178–180 °C (form A) and 159–161 °C (form B), respectively, are currently established in the literature²⁰. No studies on the crystal structures of bifendate have yet been reported. Consequently, in order to understand both the molecular conformational states in crystal lattices and their packing architectures, to investigate the reasons for polymorphism or solvatomorphism at the atomic scale, and to obtain the standard

PXRD patterns for different forms of bifendate, herein a study of the preparation and structural characterization of the bifendate polymorphs and solvatomorphs using SCXRD, thermal analysis and Fourier transform infrared spectrometry (FT-IR) was carried out. Following numerous crystallization attempts the known polymorph, form B, was produced, plus three new solvates, referred to as forms C, D, and E denoting bifendate with tetrahydrofuran, dioxane, and pyridine, respectively, in 1:1 molar ratios. SCXRD confirmed that the molecular conformations were different among distinct forms of bifendate and the simulated PXRD patterns of four forms were calculated followed by the crystallographic data of forms B–E. This provided some scientific basis for the formation of bifendate polymorphs.

2. Materials and methods

2.1. Materials

Bifendate (white powder, C₂₀H₁₈O₁₀, MW 418.36, ≥ 99.6%) was purchased from Hubei Jianyuan Chemical Engineering Inc. (Batch No. 20100707, Hubei, China) and used without further purification. All reagents used for this study were of analytical grade and purchased from Sinopharm Chemical Reagent Company Ltd. (Shanghai, China). Demineralized distilled water was used to prepare buffers.

2.2. Preparation of samples

Bifendate crystalline form B and crystallo-solvates with tetrahydrofuran (C), dioxane (D) and pyridine (E) were obtained from the filtered acetonitrile–water mixture (3.5:1, v/v), tetrahydrofuran, dioxane–water mixture (3:1, v/v) and pyridine solutions, respectively, by slow evaporation at ambient conditions after 10, 4, 6 and 20 days, respectively.

2.3. General techniques

2.3.1. Single-crystal X-ray diffraction (SCXRD)

The X-ray diffraction experiments were carried out on a Rigaku MicroMax-002+ CCD diffractometer with CuK α radiation ($\lambda=1.54178$ Å) at 293 K (Rigaku, Americas, the Woodlands, Texas, USA). Absorption correction and integration of the collected data were handled using the CrystalClear software package (Rigaku Americas). The crystal structures were solved by the direct method followed by Fourier syntheses with SHELXS-97 and then refined by full-matrix least-squares

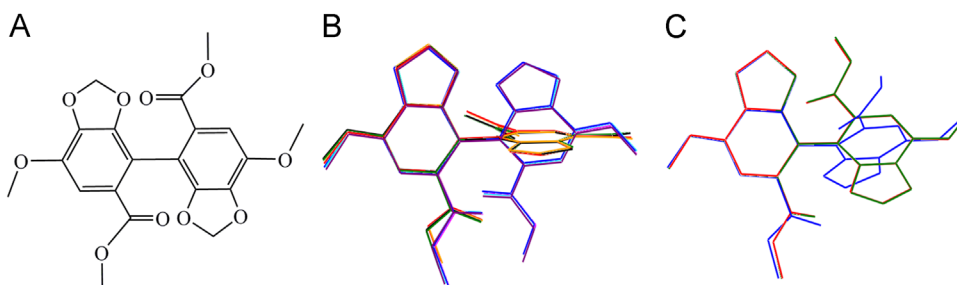


Figure 1 Chemical structure and structural overlay for forms B–E of bifendate. Eight molecules of form B are in different colors, solvate C is in red, solvate D is in blue, solvate E is in green. (A) Chemical structure of bifendate; (B) overlay of eight molecules of form B; (C) overlay of solvates C–E.

procedures using SHELXL-97 on F^2 with anisotropic displacement parameters (ADPs) for non-hydrogen atoms. The H atoms were placed in calculated positions and included in the final cycles of refinement in the riding modes²¹. To help data convergence, some restraints were introduced to the refinement of disorders²². The PLATON program with the probe radius of 1.2 Å was also employed to calculate the volume of the channels where the solvents resided in an asymmetric unit of solvates²³.

2.3.2. Calculation of powder X-ray diffractometric patterns

The MERCURY software (version 3.3, Cambridge crystallographic data center, Cambridge, UK)²⁴, with the conditions of start angle, 3° stop angle, 40° step size, 0.02°, was adopted to calculate the simulated powder X-ray pattern for a $\text{CuK}\alpha$ radiation.

2.3.3. Thermal analysis

To investigate the stoichiometry between the guests and the hosts for solvates, thermal gravimetric analysis (TGA) was performed on a Mettler Toledo DSC/TGA 1 calorimeter (Mettler Toledo, Greifensee, Switzerland). Approximately 10 mg of the sample was added to an aluminum oxide cell and heated over the temperature range of 30–500 °C at a constant heating rate of 10 °C/min and purged with a stream of flowing dry nitrogen throughout the experiment at 50 mL/min.

To better understand the thermal events, differential scanning calorimetry (DSC) was also introduced to monitor the desolvation process and determine the melting temperature of corresponding

solvates using a Mettler Toledo DSC 1 calorimeter (Mettler Toledo) with the STARe software package (Mettler Toledo) for Microsoft Windows. The samples were weighed into perforated aluminum sample pans (40 μL) and heated at the rate of 10 °C/min from 30 to 200 °C.

2.3.4. FT-IR spectroscopy

FT-IR spectra were recorded with a PerkinElmer Spectrum 400 FT-IR spectrophotometer (PerkinElmer, Waltham, Massachusetts, USA) using an attenuated total reflectance sampling accessory in the scan range of 650–4000 cm^{-1} with a resolution of 4 cm^{-1} , and then processed via the SPECTRUM software suite (PerkinElmer).

3. Results

3.1. Crystal structure

As internationally recognized, SCXRD can provide precise structural information for polymorphic compositions about molecular conformations, spatial arrangements of molecules and the way that molecules interact. To acquire the relevant information for different forms of bifendate, SCXRD was used to characterize forms B–E. Crystal data and refinement conditions for form B to E are summarized in Table 1. In all four forms, the molecular conformations were comparable, comprising two essentially planar units with the planes linked by the C–C bond of biphenyl group.

Table 1 Crystallographic data and experimental details for four crystalline forms of bifendate.

Parameter	Form B	Form C	Form D	Form E
Empirical formula	$\text{C}_{20}\text{H}_{18}\text{O}_{10}$	$\text{C}_{20}\text{H}_{18}\text{O}_{10} \cdot \text{C}_4\text{H}_8\text{O}$	$\text{C}_{20}\text{H}_{18}\text{O}_{10} \cdot \text{C}_4\text{H}_8\text{O}_2$	$\text{C}_{20}\text{H}_{18}\text{O}_{10} \cdot \text{C}_5\text{H}_5\text{N}$
Molecular weight (Da)	418.36	490.45	506.45	497.44
Crystal system	Triclinic	Orthorhombic	Orthorhombic	Orthorhombic
Space group	$P \bar{1}$	$P na_2_1$	$P 2_1 2_1 2_1$	$P na_2_1$
Color/shape	Colorless/Prism	Colorless/Prism	Colorless/Prism	Colorless/Prism
Crystal size (mm^3)	$0.45 \times 0.60 \times 0.79$	$0.19 \times 0.27 \times 0.61$	$0.39 \times 0.78 \times 0.83$	$0.59 \times 0.76 \times 0.99$
Temperature (K)	293(2)	293(2)	293(2)	293(2)
a (Å)	16.305(3)	8.516(2)	8.473(3)	8.555(2)
b (Å)	16.312(3)	21.957(4)	12.529(3)	22.243(4)
c (Å)	29.042(6)	12.429(2)	22.728(5)	12.207(2)
α (°)	97.68(3)	90.00	90.00	90.00
β (°)	97.64(3)	90.00	90.00	90.00
γ (°)	90.03(3)	90.00	90.00	90.00
Volume (Å ³)	7,586(3)	2,324.0(8)	2,412.8(12)	2,322.8(8)
Z	16	4	4	4
d_{calcd} (g/cm^3)	1.465	1.402	1.394	1.422
$F(0\ 0\ 0)$	3,488	1,032	1,064	1,040
Absorption coefficient (mm^{-1})	1.023	0.950	0.965	0.943
Theta range for data collection (°)	1.55–72.65	4.03–72.21	3.89–71.72	3.97–71.97
Reflections collected	107,349	12,118	14,611	14,776
Independent reflections	28,817	3,871	4,521	3,291
R_{int}	0.0933	0.0487	0.0623	0.0636
$R_1 [I > 2\sigma(I)]$	0.0654	0.0530	0.0454	0.0522
$wR_2 [I > 2\sigma(I)]$	0.1571	0.1445	0.1149	0.1279
R_1 (all)	0.0904	0.0579	0.0482	0.0535
wR_2 (all)	0.1765	0.1533	0.1190	0.1299
Goodness-of-fit on F^2	0.998	1.045	1.059	1.064
Completeness	0.956	0.990	0.986	0.978
CCDC deposition number	1,432,083	1,432,084	1,432,085	1,432,086

Additionally, the molecular arrangement mode was also considered together with intermolecular interactive mode, and the simulated PXRD patterns of the four forms were calculated.

SCXRD analysis revealed that form B of bifendate belonged to $P\bar{1}$ space group, triclinic crystal system while solvates C and E crystallized in the orthorhombic space group $Pna2_1$, $P2_12_12_1$, and $Pna2_1$, respectively. Form B was a non-solvated polymorph, with the asymmetric unit composed of 8 molecules, and 16 molecules located in the unit cell. The basic molecular skeleton for bifendate was a biphenyl structure, consisting of 2 symmetrical fragments, in which both of the 5- and 6-membered rings were almost planar and coplanar. The guest solvent molecules of solvate C–E were tetrahydrofuran, dioxane and pyridine, respectively, in stoichiometry 1:1 with the host molecule. For the three solvates, the basic unit contained one bifendate molecule and one solvent molecule, which had a higher temperature factor because of the disordered thermal motion of the solvent molecule. The dihedral angles between two planar fragments linked by the C–C bond of the biphenyl group of forms B–E are shown in Table 2, which displayed obvious differences among the four forms.

The crystal density value of form B was higher than those of forms C to E, illustrating that the bifendate molecules were arranged tightly in three-dimensional space, and the calculated volume (103.7 \AA^3) of solvent-accessible voids per the unit-cell volume in form B was 1.4%. Comparing that with form B, it was easy to see that all the molecules in the structures of forms C to E were arranged loosely with the corresponding calculated volume of 537.2 \AA^3 (C), 644.6 \AA^3 (D), and 534.9 \AA^3 (E) accounting for approximately 23.1%, 26.7%, and 23.0% of unit-cell volume.

3.1.1. Conformational analysis

Fig. 1B shows a structure overlay for form B of bifendate, with two molecules in different conformational states in an asymmetry unit, and in which the two symmetrical fragments linked by the C–C bond from the biphenyl group were not coplanar, with the corresponding torsion angles being 69.3° and -69.3° , respectively. Apart from that, and despite two methyl ester side chains in each molecule directed to the identical side owing to the single-bonding rotations, two different orientations were shown for the

Table 2 Dihedral angles between the ring planes linked by C–C bond of the biphenyl group.

Form	$\angle R_1-R_2$ ($^\circ$) ^a
B (A)	71.3
C	125.3
D	125.7
E	126.7

^a R_1 denotes the C1/C2/C3/C4/C5/O4/C16/O5/C6 ring; R_2 denotes the C7/C12/C11/C10/C9/O7/C17/O6/C8 ring.

molecules, including the methoxyl fragments. To better describe the molecular conformational state the relative torsion angles in the basic unit for the 4 forms were calculated and are listed in Table 3. Structure overlay for 3 solvates of bifendate are shown in Fig. 1C; it is clear that the host molecules also displayed 2 different molecular conformations for the solvates. Among these, the host molecules in forms C and E adopted the same conformation of the C–C bond of biphenyl group rotating outwards from the paper, with the torsion angle of $120.7(3)^\circ$ and $122.1(3)^\circ$, respectively, while that of solvate D rotated in an inward direction and the torsion angle was $-121.3(2)^\circ$. In addition, with regard to the single bond rotations, significant differences in the orientation of methyl ester and methoxyl were observed among the three solvates; several of the methoxyl fragments of form D were turned to the identical side in comparison with those in forms C and E, which were pointed to two different sides. Secondly, although a pair of methyl ester groups for each solvate were turned to the identical side, those in solvate D were discovered to adopt to the opposite orientation with respect to those of solvates C and E.

3.1.2. Intermolecular interaction

As depicted in Fig. 2, in the crystal structure of form B, non-classical hydrogen bonds and weak π - π stacking interactions played an important role in forming a supramolecular structure. The host molecules were assembled into a one-dimensional chain along the $[0\ 0\ 1]$ direction via weak π - π stacking interactions between the phenyl rings and the oxygenic heterocyclic rings. Together with the non-classical hydrogen bonds, a two-dimensional layer parallel to the $(0\ 0\ 1)$ plane can be constructed. When the non-classical hydrogen bonds and van der Waals forces were considered together, a three-dimensional supramolecular structure was completed in the crystal structure. Meanwhile, layered structures of solvates C–E with solvent molecules located in the channels between the layers for solvates C to E are shown in Fig. 3A–C. It was disclosed that the guest solvent molecules were, in turn, arranged in the channel formed by the host molecules, which resulted in a “Z” chain structure parallel to the a axis. The host molecules interacted with the guest molecules through an intercalation mode. Fig. 3D–F display a space-filling representation of bifendate showing the continuous channels along $[1\ 0\ 0]$ viewed down crystallographic a axis for the three solvates. As seen in the figure, among these solvates, channels of the forms C and E were similar but different from that of form D.

3.1.3. Simulated powder X-ray diffraction analysis

The simulated powder X-ray diffraction patterns for each form of bifendate and solvates C–E after deducting solvents based on the crystallographic data of forms B–E are given in Fig. 4. As shown, the simulated PXRD pattern for forms B–E was unique, and the topologies of PXRD patterns of solvates C to E were similar, especially for forms C and E. Three strong characteristic peaks

Table 3 Torsion angle values describing conformational states of bifendate molecules in four forms studied.

Form	$\angle C_6-C_1-C_7-C_8$	$\angle C_{15}-O_3-C_4-C_3$	$\angle C_1-C_2-C_{13}-O_1$	$\angle C_7-C_{12}-C_{19}-O_9$	$\angle C_{18}-O_8-C_{10}-C_{11}$
B (A/C)	$69.3(3)/-69.3(3)$	$-6.4(3)/5.5(3)$	$21.8(4)/-25.1(4)$	$24.4(4)/-23.5(3)$	$-3.4(3)/7.9(3)$
C	$120.7(3)$	$9.5(6)$	$-25.6(5)$	$-28.7(5)$	$-5.8(5)$
D	$-121.3(2)$	$-11.8(4)$	$27.8(3)$	$27.2(3)$	$-1.6(4)$
E	$122.1(3)$	$-7.2(5)$	$-30.2(4)$	$-25.9(4)$	$9.6(5)$

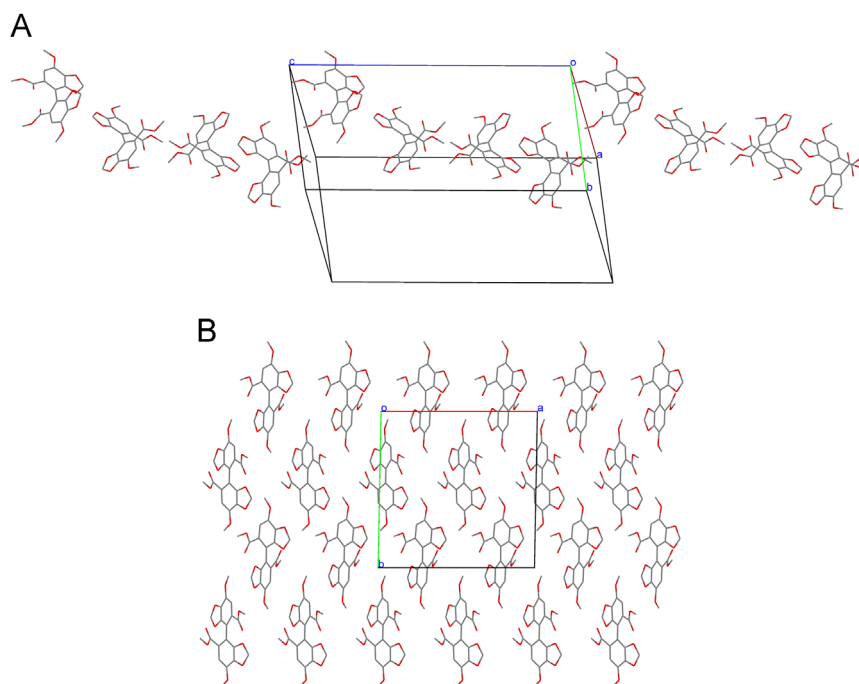


Figure 2 Stereochemical structure of form B: (A) a view of the one-dimensional catenoid structure of form B along [0 0 1] direction; (B) a view of the two-dimensional layer structure of form B along (0 0 1) plane. Molecules are shown as wireframe models and hydrogen atoms are omitted for clarity.

appeared at the 2θ range of $5\text{--}10^\circ$ and $22\text{--}28^\circ$ for forms C–E, and the values of d were 10.98, 3.67, 3.53 Å (form C); 11.36, 3.77, 3.56 Å (form D); 11.12, 3.63, 3.49 Å (form E) corresponding to the indices of lattice plane (0 2 0), (1 1 3), (1 2 3); (0 0 2), (1 2 4), (1 3 2) and (0 2 0), (1 1 3), (1 2 3), for solvates C, D, and E, respectively. The presence of characteristic peaks coincided well with the results of SCXRD. Moreover, Fig. 4B–D clearly indicates that the varying peaks for solvates C–E after deducting solvents, which can be assigned to the corresponding diffraction peaks of tetrahydrofuran, dioxane, and pyridine, respectively. Thus, the varying peaks for solvates C–E, with the d -spacings of 7.94, 6.69, 5.41, 5.07, 4.89, 4.57, 4.32, 4.14, 4.07, 3.96, 3.90, 3.78, 3.67, 3.53 Å (form C), 7.94, 5.65, 5.49, 5.15, 5.04, 4.92, 4.60, 4.42, 4.20, 4.11, 4.00, 3.95, 3.77, 3.56 Å (form D), and 7.98, 6.68, 6.33, 5.60, 5.35, 4.84, 4.35, 4.12, 3.97, 3.79, 3.70, 3.62, 3.49 Å (form E) correlated to tetrahydrofuran, dioxane, and pyridine, respectively.

3.2. Thermal analysis

To elucidate the thermodynamic behaviors of forms B, C, D, and E for bifendate, differential scanning calorimetry (DSC) and thermal gravimetric analysis (TGA) were employed to assess the thermal events. According to the results of DSC and TGA (Fig. 5), it further confirmed that, except for form B, forms C–E were all solvates. For form B, the DSC heating curve showed a single endothermic peak with a value of 162.82°C while those of solvates C–E presented double endothermic peaks. The first endothermic peak values in forms C–E were 77.21°C , 128.27°C , and 81.42°C , respectively, and the second were 182.63°C , 181.65°C , and 182.11°C , respectively. The DSC data for forms B–E of bifendate are listed in Table 4. The weight loss of solvents for solvates C, D, and E of bifendate by TGA were 14.57%, 17.13%, and 15.13%, respectively, corresponding to the

number of the solvent in each asymmetry unit of solvates of 0.99, 0.98, and 0.96, respectively, which was in agreement with the results of SCXRD.

3.3. IR spectra

With the purpose of further clarifying the distinctions between the different polymorphs, the FT-IR spectra for forms B–E of bifendate were studied and assigned on the basis of a careful comparison between crystalline form B and solvates. As illustrated in Fig. 6, it was noteworthy that the band appearing at 737 cm^{-1} was the specialized absorption band for form B used to distinguish from form A but not seen in other solvates²⁰, which was in accord with the study of DSC. Comparing with form B, it can be found that the intensity of the bending vibration of the C–H bond from the methylene group (1464 cm^{-1}), together with the stretching vibration of the C–O bond from methoxyl group (1262 cm^{-1}) decreased sharply in solvates C and E, while that in solvate D almost disappeared. In addition, the band associated with the $\delta_{\text{C-C}}$ presenting at 1136 cm^{-1} in form B was shifted considerably toward lower frequency at 1119 cm^{-1} in form D and was hardly evident in solvates C and E. Lastly, an apparent distinction in the fingerprint region with the range of $1000\text{--}850\text{ cm}^{-1}$ for all the four forms was also observed.

4. Discussion

Based on the results of SCXRD, form B was a non-solvated polymorph and forms C–E were solvates. The different space groups illustrated that the molecular symmetry was different between the non-solvated form and the three solvates. As seen in Table 1, the densities of solvates C–E were lower than that of form B, which indicated the molecules in the structures of forms

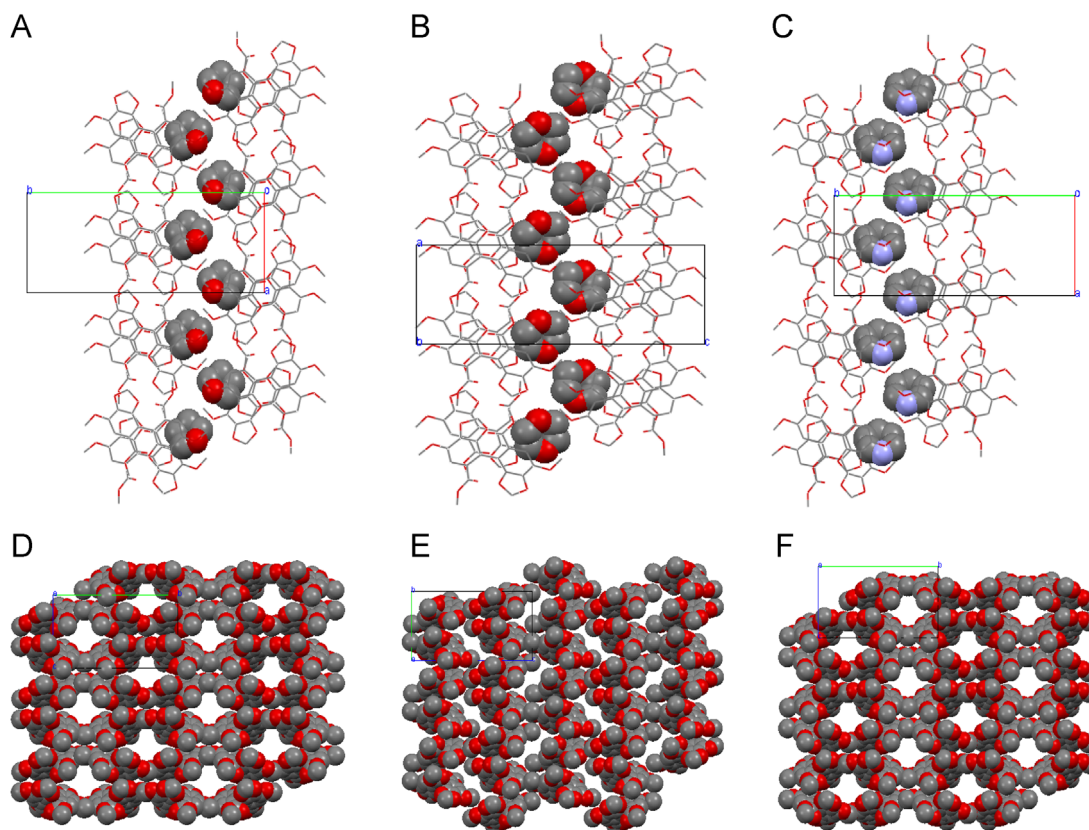


Figure 3 Upper row: layered structures of solvates C–E with solvent molecules located in the channels between the layers for (A) solvate C: tetrahydrofuran, view down c axis; (B) solvate D: dioxane, view down b axis; (C) solvate E: pyridine, view down c axis. Solvent molecules are represented by spheres corresponding with the van der Waals radii of the respective atoms. Hydrogen atoms are omitted for clarity. Lower row: space-filling representation of bifendate showing the continuous channels along $[1\ 0\ 0]$ viewed down crystallographic a axis for (D) solvate C: tetrahydrofuran; (E) solvate D: dioxane and (F) solvate E: pyridine. Bifendate molecules are represented by spheres corresponding with the van der Waals radii of the respective atoms. Solvents are omitted for clarity.

C–E are arranged loosely, and also demonstrated indirectly the greater thermodynamic stability of form B relative to forms C–E. Furthermore, the larger calculated volumes of solvent-accessible voids per the unit-cell volume in solvates C–E implied that big molecular channels may exist in the stereochemical structure to hold the solvents molecules for the three solvates.

In the structure of form B, the benzene rings of the biphenyl group connect with each other in a skew-skew fashion; this led to two symmetrical fragments linked by the C–C bond of the biphenyl group and resulted in two different conformational molecules presented in an asymmetry unit. For the diversity of the molecular conformation, eight bifendate molecules were assembled into an asymmetry unit for form B. In comparison with form B, two different molecular conformations were also found for solvates C–E; however, because of the adducted solvents, the C–C bond further rotated and the torsion angle increased, resulting in two molecular conformations that were different from that in form B. These adducted solvents had an important influence on the conformations of host molecules.

The interactions of the guest with the host evoked our interest. Theoretically speaking, neither the host molecules nor the guest molecules contained potentially strong hydrogen bond donors or acceptors capable of interacting by classical hydrogen bonds in solvates C–E. In spite of some rigid and planar phenyl rings present in the host molecules, neither the saturated 5-membered ring tetrahydrofuran molecules nor the 6-membered ring dioxane

molecules could interact with host molecules by π - π stacking interactions, while the minimum centroid–centroid separation of $4.340(3)$ Å was too far for the pyridine rings to generate aromatic π - π stacking interactions with the phenyl rings of the host. In fact, as the structure of form B showed, a dihedral angle of approximately 71° between the two planar fragments existed in the host molecule because of the rotation of the C–C bond in the biphenyl skeleton. All the guest solvent molecules for forms C, D, and E involving tetrahydrofuran, dioxane, and pyridine, respectively, were planar with suitable volumes, and could be available to insert into the gap formed by two bifendate molecules. The four host molecules formed a large cavity in which two guest molecules could reside through intercalative interactions, with the host molecules stabilized by weak π - π stacking interactions and non-classical hydrogen bonds to form a molecular channel, where the guest molecules arranged by turns forming a “Z” chain structure as described above. The intercalation mode between guest and host molecules gave rise to further rotation of the C–C bond and resulted in the dihedral angle increasing, with the corresponding value of 125.3° (form C), 125.7° (form D), and 126.7° (form E).

On these grounds, we deduced that to incorporate into the channel formed by the host molecules, guest molecules should meet some structural requirements: on one hand, the guest molecules should be planar so that they could insert into the gap assembled by the host molecules; on the other hand, the expected volumes of the guests should be 100 – 300 Å³ to maintain the

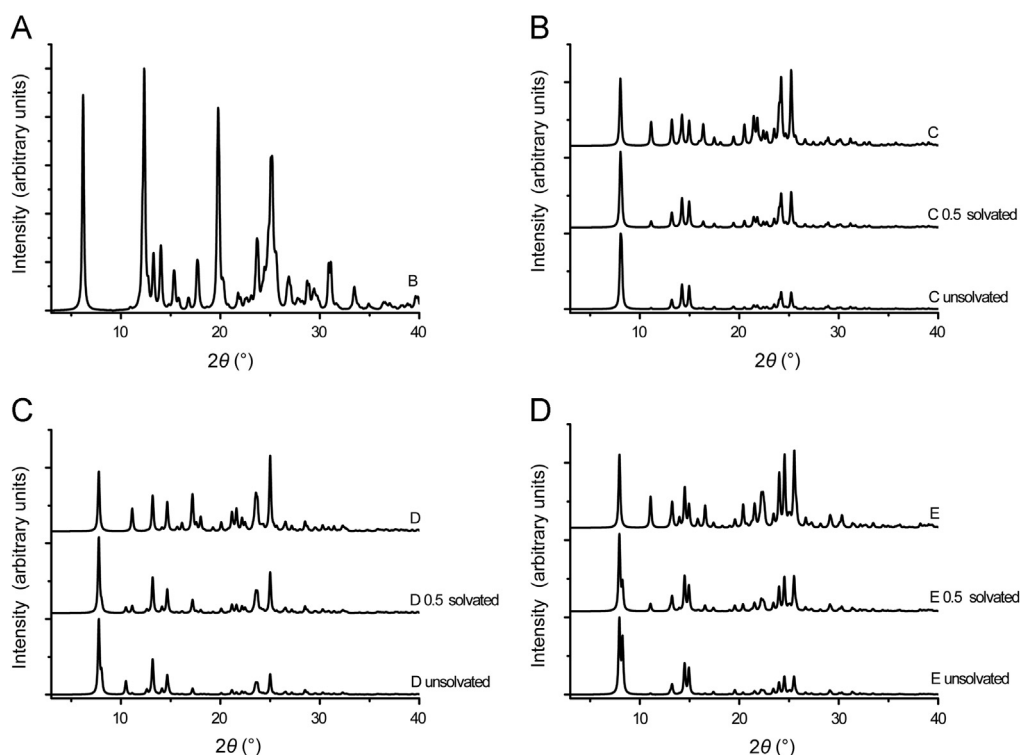


Figure 4 Simulated PXRD pattern for form B and comparison of the simulated PXRD patterns for solvates C–E and those after deducting solvents of bifendate. (A) form B; (B) solvate C: tetrahydrofuran; 0.5 solvated; unsolvated; (C) solvate D: dioxane; 0.5 solvated; unsolvated; (D) solvate E: pyridine; 0.5 solvated and unsolvated.

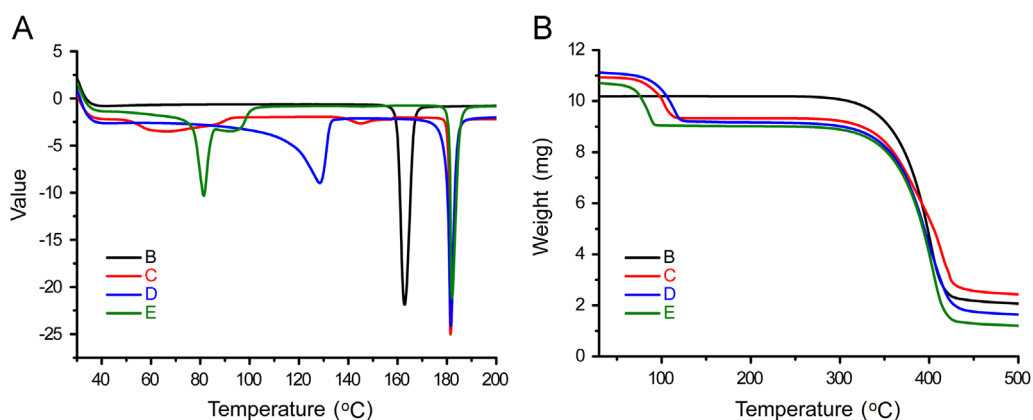


Figure 5 Thermal analysis profiles of forms B–E. (A) DSC profiles of forms B–E; (B) TGA profiles of forms B–E. Profiles of forms B–E are indicated with black, red, blue, and green, respectively. Top to bottom: form B; solvate C: tetrahydrofuran; solvate D: dioxane; and solvate E: pyridine.

stability of the molecular structures. This explains why we could not generate additional solvates with small molecules such as methanol or ethanol.

The simulated powder X-ray diffraction analysis showed that the simulated PXRD patterns of forms B to E were unique and the patterns of all the solvates after deducting the solvents were also very different. The stated analysis showed that the main differences between the four forms were the solvents, the molecular arrangements and the modes of interaction, which led to the

Table 4 DSC data for forms B–E of bifendate.

Form	T_{desolv} (°C, peak)	T_{fus} (°C, peak)
B	–	162.82
C	77.21	182.63
D	128.37	181.65
E	81.42	182.11

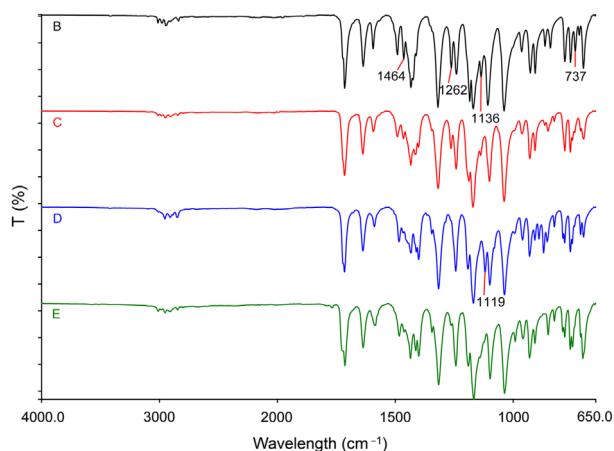


Figure 6 Infrared spectra for forms B to E of bifendate with scanning region of 4000–650 cm^{-1} . Spectra of forms B to E are indicated with solid lines in black, red, blue, and green, respectively. Top to bottom: form B; solvate C: tetrahydrofuran; solvate D: dioxane; and solvate E: pyridine.

differences in the simulated PXRD patterns of forms B–E. Furthermore, the simulated PXRD patterns of all the solvates after deducting solvents may allow prediction of other new polymorphs for bifendate. In the DSC profiles, the T_{fus} value of form B was 162.82 °C and was in agreement with its reported melting point, which confirmed that form B was a pure non-solvated polymorph. Among the double endothermic peaks for solvates C–E, the first melting peak can be attributed to that of the solvent while the second was the endothermic peak of polymorph, with the T_{fus} value of 182.63 °C (form C), 181.65 °C (form D), and 182.11 °C (form E), respectively, consistent with the reported melting point of form A. This indicated that the three solvates could be transformed into form A under suitable temperature conditions because of its greater thermodynamic stability, which was confirmed by desolvation. The differences of the FT-IR spectra for forms B–E of bifendate indicated that the incorporation of solvents could affect the molecular arrangement and intermolecular interaction mode, and resulted in the changes of the infrared absorption spectra.

5. Conclusions

Our study demonstrates that bifendate has the characteristic of solvatomorphism. Crystalline form B and three new solvates of bifendate with structurally similar solvent molecules were obtained and their crystal structures were characterized. By comparing the crystal structures of form B with the three solvates C–E, it can be concluded that, firstly, weak π - π stacking interactions and non-classical hydrogen bonds made an important contribution to the three-dimensional supramolecular structures for the four forms; secondly, the rotation of the C–C bond of the biphenyl group together with methyl ester and methoxyl fragments led to distinct molecular conformations in crystal lattices, which may result in 8 bifendate molecules per asymmetry unit for form B; thirdly, all the guest solvent molecules interacted with the host molecules through an intercalation pathway arranged by turns in the channel formed by the host molecules; lastly, the incorporation of the guest solvent molecules had an important influence on the host molecular conformation. Consequently, we conclude that the guest

molecules should be planar with the expected volumes of approximately 100–300 \AA^3 to interact with the bifendate molecules. Moreover, all the three solvates were unstable under high temperature conditions. SCXRD analysis illustrated that adducted solvents, the differences in the molecular conformation and the spatial arrangement caused the formation of polymorphs of bifendate. In addition, the unique simulated powder X-ray diffraction patterns were calculated from single crystal experiments of forms B–E and provided a standard for identifying the purity of polymorphs and solvates. Further investigations on this and similar systems are in progress in our laboratory.

Acknowledgments

We thank the Ministry of Science and Technology of the People's Republic of China for the National Science (Grant No. 2012ZX09301002-001-013).

References

- Surov AO, Solanko KA, Bond AD, Bauer-Brandl A, Perlovich GL. Crystal architecture and physicochemical properties of felodipine solvates. *CrystEngComm* 2013;**15**:6054–61.
- Pudipeddi M, Serajuddin ATM. Trends in solubility of polymorphs. *J Pharm Sci* 2005;**94**:929–39.
- Henwood SQ, Liebenberg W, Tiedt LR, Lätter AP, de Villiers MM. Characterization of the solubility and dissolution properties of several new rifampicin polymorphs, solvates, and hydrates. *Drug Dev Ind Pharm* 2001;**27**:1017–30.
- Li ZJ, Abramov Y, Bordner J, Leonard J, Medek A, Trask AV. Solid-state acid-base interactions in complexes of heterocyclic bases with dicarboxylic acids: crystallography, hydrogen bond analysis, and ^{15}N NMR spectroscopy. *J Am Chem Soc* 2006;**128**:8199–210.
- Heinz A, Strachan CJ, Gordon KC, Rades T. Analysis of solid-state transformations of pharmaceutical compounds using vibrational spectroscopy. *J Pharm Pharmacol* 2009;**61**:971–88.
- Brittain HG. Polymorphism and solvatomorphism 2010. *J Pharm Sci* 2012;**101**:464–84.
- Byrn SR. In: *Solid-state chemistry of drugs*. 2nd ed. West Lafayette: SSCI Inc.; 1999.
- Griesser UJ. The importance of solvates. In: Hilfiker R, editor. *Polymorphism: in the Pharmaceutical Industry*. Weinheim: Wiley-VCH; 2006.
- Cains PW. Classical methods of preparation of polymorphs and alternative solid forms. In: Brittain HG, editor. *Polymorphism in Pharmaceutical Solids*. 2nd ed. New York: Informa Healthcare; 2009.
- Benigni DA, Gougoutas JZ, DiMacro JD, inventors; Bristol-Myers Squibb Co., assignee. Paclitaxel solvates. US patent 6858644. 2005 February 22.
- Didier E, Perrin MA. Dimethoxy docetaxel acetone solvate et method for the preparation thereof. Patent WO2005/028462 A1. 2005 March 31.
- Xie JX, Zhou J, Zhang CZ, Yang JH, Chen JX. Synthesis of schizandrin C analogs. *Acta Pharm Sin* 1981;**16**:306–9.
- El-Beshbishy HA. The effect of dimethyl dimethoxy biphenyl dicarboxylate (DDB) against tamoxifen-induced liver injury in rats: DDB use is curative or protective. *J Biochem Mol Biol* 2005;**38**:300–6.
- Kim SN, Kim SY, Yim HK, Lee WY, Ham KS, Kim SK, et al. Effect of dimethyl-4,4'-dimethoxy-5,6,5',6'-dimethylenedioxybiphenyl-2,2'-dicarboxylate (DDB) on chemical-induced liver injury. *Biol Pharm Bull* 1999;**22**:93–5.
- Liu GT, Wei HL, Song ZY. Further studies on the protective action of biphenyl dimethyl-dicarboxylate (BDD) against experimental liver injury in mice. *Acta Pharm Sin* 1982;**17**:101–6.

16. Pan SY, Yang R, Dong H, Yu ZL, Ko KM. Bifendate treatment attenuates hepatic steatosis in cholesterol/bile salt- and high-fat diet-induced hypercholesterolemia in mice. *Eur J Pharm* 2006;**552**:170–5.
17. Liu MH, Zhao LS, Yang D, Ma J, Wang XL, Zhang TH. Preclinical pharmacokinetic evaluation of a new formulation of a bifendate solid dispersion using a supercritical fluid chromatography–tandem mass spectrometry method. *J Pharm Biomed Anal* 2014;**100**:387–92.
18. Gu XK, Ren ZG, Peng H, Peng SX, Zhang YH. Bifendate-chalcone hybrids: a new class of potential dual inhibitors of P-glycoprotein and breast cancer resistance protein. *Biochem Biophys Res Commun* 2014;**455**:318–22.
19. Gu XK, Ren ZG, Tang XB, Peng H, Ma YF, Lai YS, et al. Synthesis and biological evaluation of bifendate-chalcone hybrids as a new class of potential P-glycoprotein inhibitors. *Bioorg Med Chem* 2012;**20**:2540–8.
20. Wang ZH, Yang YG. DSC determination of bifendate polymorphism. *Chin J Pharm Anal* 2010;**30**:2101–3.
21. Sheldrick GM. A short history of *SHELX*. *Acta Cryst A* 2008;**64**:112–22.
22. Müller P, Herbst-Irmer R, Spek AL, Schneider TR, Sawaya MR. *Crystal structure refinement*. New York: Oxford University Press Inc.; 2006.
23. Spek AL. Structure validation in chemical crystallography. *Acta Cryst D* 2009;**65**:148–55.
24. Macrae CF, Edgington PR, McCabe P, Pidcock E, Shields GP, Taylor R, et al. Mercury: visualization and analysis of crystal structures. *J Appl Cryst* 2006;**39**:453–7.